

HTS Bandstop Filter for Radio Astronomy

Srikanta Pal, *Member, IEEE*, Michael J. Lancaster, *Senior Member, IEEE*, and Roger D. Norrod, *Member, IEEE*

Abstract—A novel miniaturized six-pole high temperature superconducting microstrip bandstop filter operating at S band is presented in this letter. A pseudo elliptical behavior in the frequency characteristic is introduced by designing the resonators to resonate at asynchronous frequencies and by varying the inter resonator phase difference. These filters have been installed in a cryogenic radio astronomy receiver with excellent results. Because of their sharp cut-off characteristics, the filters reduce satellite downlink interference signals by more than 40 dB while minimizing lost observing bandwidth.

Index Terms—Bandstop filter, high temperature superconducting (HTS), meanderline open loop resonator, radio astronomy.

I. INTRODUCTION

MOST radio astronomy receivers use cryogenic cooling to achieve the best possible noise performance and sensitivity. The National Radio Astronomy Observatory (NRAO) Robert C. Byrd Green Bank Telescope located in West Virginia provides a suite of up to nine remotely selectable cryogenic receivers, each optimized for specific portions of the 0.3–100 GHz operating range of the antenna. One of these, the S-band receiver, operates at 1.73–2.60 GHz and is heavily used for pulsar and planetary radar observations. This frequency range encompasses downlink bands used by Satellite Digital Audio Radio Services (SDARS) satellites and the SDARS signals were typically seen more than 20 dB above the system noise floor even with the telescope pointing well away from the geosynchronous satellite band. While not usually causing overload of the first cryogenic amplifiers, the signals propagated throughout the system and caused inter-modulation products and ringing in later stages. Use of conventional filters to attenuate the interfering signals caused more lost observing bandwidth than was desired, so it was decided to investigate the use of superconducting notch filters with their potential of higher Q and steeper rejection skirts.

Low loss materials are critical to the design of high performance filters. The minimization of dissipative losses in radio astronomy receivers is a never-ending engineering task [1]. Small resistive losses also degrade the quality of frequency-selective filters needed to reject strong interference. In this regard, higher

TABLE I
SPECIFICATIONS FOR HTS S-BAND NOTCH FILTER

passband	1700 MHz–2700 MHz (excluding of notch)
notch rejection band	2320 MHz–2345 MHz
notch rejection	40 dB minimum
notch 1 dB bandwidth	40 MHz maximum
passband VSWR	1.25:1 max (exclusive of notch)
phase Match (2 units)	+/- 5 deg

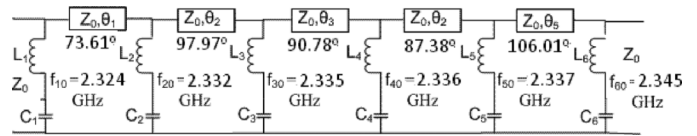


Fig. 1. Equivalent circuit of the bandstop filter, where Z_p is the characteristic impedance of the phase line, θ_n is the electrical length.

Q and steep roll off that are achievable by using HTS filters is unrivalled by any other material. In this letter, the design of a novel HTS six-pole microstrip pseudo elliptic bandstop filter is described.

II. BANDSTOP FILTER DESIGN

The specification of the S-band HTS bandstop filter is shown in Table I. The proposed filter is a 6 –pole pseudo elliptic microstrip bandstop filter.

The design here is based on a Chebyshev prototype bandstop filter in which the circuit component values can be calculated [2]. This circuit is then converted to a pseudo elliptic bandstop filter using optimization in a circuit simulator to adjust the resonant frequencies and the phase lengths between resonators. The equivalent circuit of the optimized filter in the lumped element ladder network form, is shown in Fig. 1.

A superconducting microstrip L band notch filter design for radio astronomy application has been reported earlier [3], [5]. However, in this letter, the quasi-elliptic method of design is investigated further, with the design of an even order filter at higher centre frequency and wider stop band width. The use of the filter in a radio astronomy application is also reported. Using this method, we were able to reduce the number of resonators required to meet the specifications by two, as compared with a Chebyshev response, thereby reducing the volume of the filter.

In the case of a Chebyshev bandstop filter design, the resonant frequency of each of the resonators is same, and the phase length between any two resonators is equal to $\lambda/4$. For the design of a pseudo elliptic bandstop filter [4], the phase lengths vary from $\lambda/4$ and the resonant frequency of the series resonators may also be unequal, as shown in Fig. 1.

Manuscript received December 21, 2011; accepted March 20, 2012. Date of publication April 16, 2012; date of current version May 04, 2012. This work was supported by the U.K. Engineering and Physical Sciences Research Council.

S. Pal is with the Department of Electronics and Communication Engineering, Birla Institute of Technology, Mesra, Ranchi – 835215, India (e-mail: pal_srikanta@yahoo.co.uk).

M. J. Lancaster, is with the Department of Electronics, Electrical and Computer Engineering, University of Birmingham, Edgbaston, Birmingham B15 2TT, U.K. (e-mail: m.j.lancaster@bham.ac.uk).

R. D. Norrod is with the National Radio Astronomy Observatory, Green Bank, WV 24944 USA (e-mail: rnorrod@nrao.edu).

Digital Object Identifier 10.1109/LMWC.2012.2193122

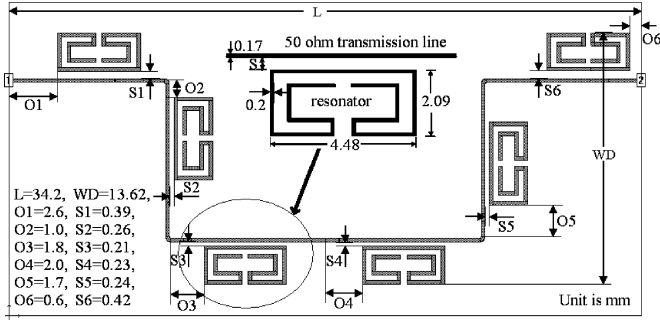


Fig. 2. Layout of the 6-pole microstrip HTS bandstop filter.

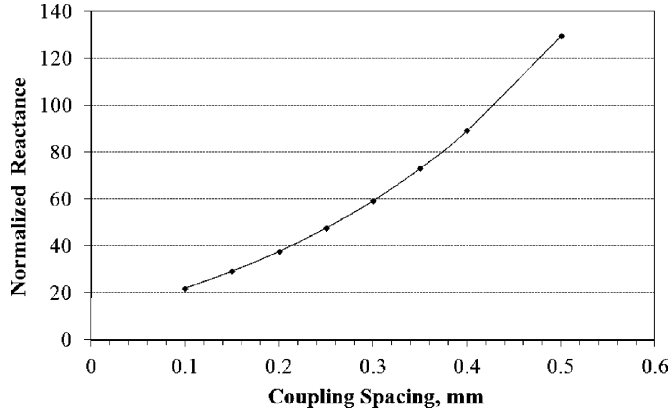
Fig. 3. Normalized reactance slope parameters, x/Z_0 versus coupling spacing, s .

Fig. 2 shows the layout of the microstrip filter. The problem is to determine the positioning of the resonators based on the circuit in Fig. 1. The gap between the transmission line and the resonator can be found by considering the reactance slope parameter, which can be defined in terms of low-pass prototype elements [2]

$$x_i = \omega_i L_i = \frac{1}{\omega_i C_i} = Z_0 \frac{g_0}{g_i FBW} \quad \text{for } i = 1 \text{ to } n \quad (1)$$

here ω_i represents the resonant frequency of each of the resonators and are not all the same. FBW is the stopband fractional bandwidth. The relationship between x_i and the frequency response of the bandstop filter is [2]

$$\frac{x_i}{Z_0} = \frac{f_0}{2\Delta f_{i3 \text{ dB}}} \quad \text{for } i = 1 \text{ to } n \quad (2)$$

where f_0 is the center frequency and $\Delta f_{i3 \text{ dB}}$ is the 3 dB rejection bandwidth. By simulating single resonators coupled to a transmission line, and noting the centre frequency and 3 dB bandwidth, a relationship can be built up of x/Z_0 against the spacing of the resonator with respect to the transmission line. This is shown in Fig. 3. With this information the dimensions of the resonators, the spacing between them, as well as the gap to the transmission line are all defined. To fine tune the result, all dimensions are further optimized in a full wave electromagnetic simulator. The results are shown in Fig. 4(a).

The asynchronous resonators are realized using varying length of transmission line which is folded inward in a zig-zag

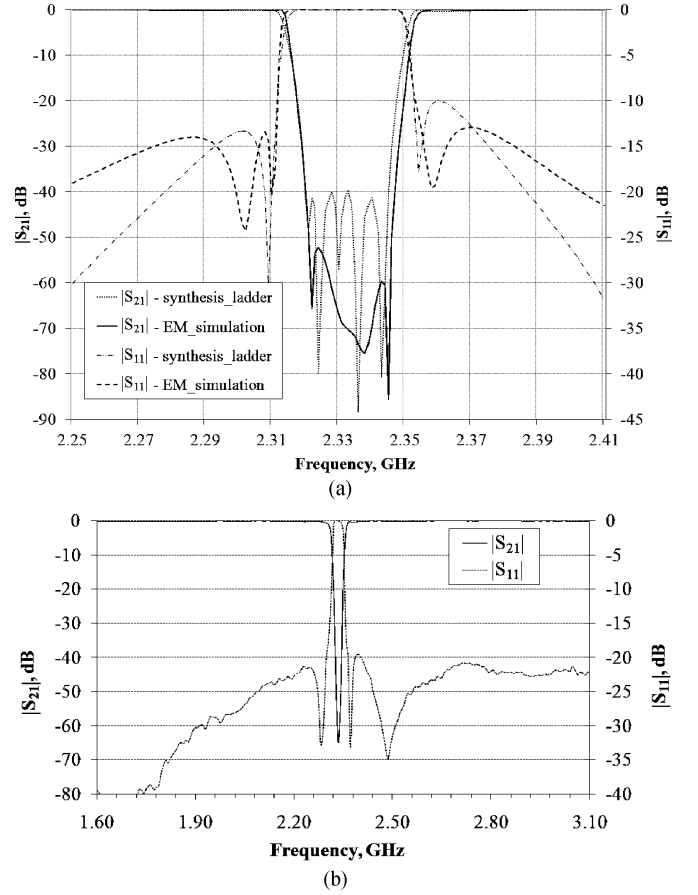


Fig. 4. (a) Narrowband frequency response of the six-pole HTS bandstop filter using circuit synthesis and electromagnetic simulation, (b) Simulated wideband performance of the six-pole HTS microstrip bandstop filter (thin solid line - $|S_{21}|$ (dB); thin dash line - $|S_{11}|$ (dB)).

fashion, leaving a large loop in the middle of the line. On a 0.508 mm thick LaAlO_3 substrate (relative dielectric constant $\epsilon_r = 23.6$) the width of the 50 Ω transmission line is 0.17 mm.

Radiation coupling from one resonator to the other is reduced because electric current at any two symmetrical positions flows in opposite directions. Therefore, both the strong electric field at the open ends and the strong magnetic field at the middle of the resonator are reduced by the opposite current flow in the inward zig-zag lines. This allows resonators to be placed in a relatively small area without substantial unwanted coupling [3]. Due to packaging constraints, the size of the filter is restricted to less than 2 inches. This was achieved by meandering the 50 Ω transmission line into a 2-leg zig-zag, as depicted in Fig. 2.

The comparison of synthesized and EM simulated frequency characteristics of the filter with the circuit model are shown in Fig. 4(a). The difference in the synthesized and EM simulated response is found to be an upward shift of 1.5 MHz in case of the synthesized response. Six nulls in the stopband part of synthesized transmission response are visible, whereas only three nulls are visible in the EM simulated the response. The simulated wideband frequency characteristics are shown in Fig. 4(b) [6].

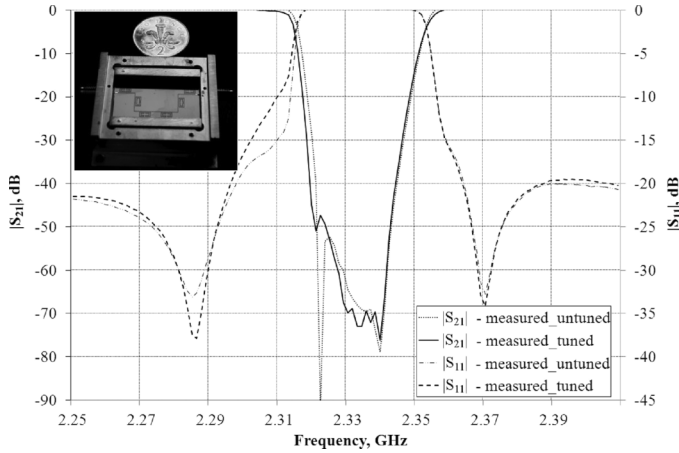


Fig. 5. HTS notch filter's measured attenuation and reflection characteristics before tuning and after tuning. The photograph of the fabricated filter is in the inset.

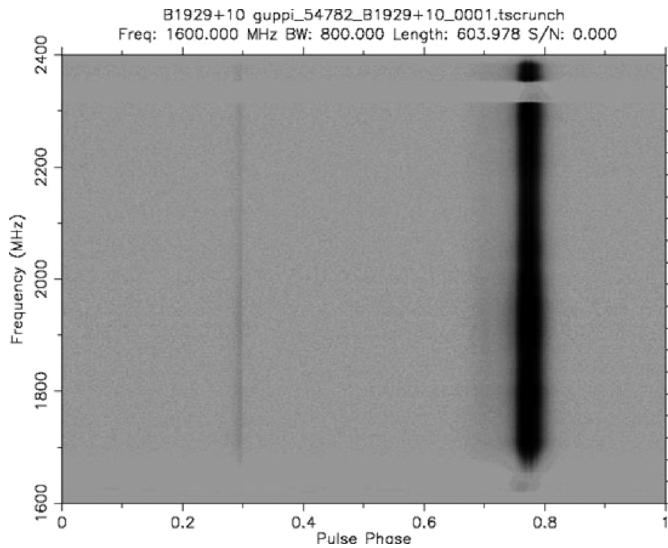


Fig. 6. Dynamic pulsar spectrum of pulsar B1929+10 showing the sharp frequency band removed by the HTS notch filter near the top of the image [1]. The horizontal scale is normalized to the pulsar period, about 220 msec in this case. The signal intensity is indicated by the linear gray scale.

A. Fabrication and Results

The HTS microstrip bandstop filter was fabricated using YBCO thin film of 600 nm thickness on a 0.508 mm thick LaAlO_3 substrate. The filter circuit is etched using ion beam milling. The circuit was mounted on a gold-plated titanium carrier, which was fixed into a gold plated titanium box. The titanium housing of the filter is $1.7 \times 4.0 \times 4.7$ cm.

The measured performance of the filter at 24 K is shown in Fig. 5. The figure shows the comparison of the measured-tuned and measured untuned frequency characteristics of the bandstop filter. Tuning was done with the help of sapphire and metal tuning screws placed over the resonators. The tuned passband insertion loss is 0.15 dB, and the return loss is better than 15 dB in the passband of the filter. The measured response shows a 3 MHz narrower 40 dB rejection bandwidth before tuning.

With respect to the centre frequency at 2.3325 GHz, the filter is tuned to the desired requirement of 25 MHz bandwidth at 40 dB rejection and 40 MHz bandwidth at 1 dB rejection.

Other performance parameters as mentioned in Table I are measured in NRAO and results of these measurements can be found in [7]. A dynamic pulsar spectrum, as observed after these filters were installed in the GBT receiver, is shown in Fig. 6. The detected frequency range is determined by the cryogenic receiver and data backend equipment limitations, as well as the need for an interference-free spectrum. The dark vertical stripe is the main pulsar pulse; the faint vertical stripe is the pulsar inner pulse. Removal of the SDARS interference by the notch filter allows an increase in detection bandwidth of about 10% and corresponding improvement in sensitivity or reduction in required observing time [8].

III. CONCLUSION

A novel six-pole HTS microstrip elliptic bandstop filter at S band has been presented. The extremely low loss required for the sharp filter characteristics shown in Fig. 5 is not achievable with normal metal conductors. Resonators with different resonant frequencies connected with different phase lengths produce pseudo elliptical characteristics after which helps in reducing the number of resonators (by two over the case of Chebychev response). These filters are installed after the cooled amplifiers in the NRAO GBT S-band receiver, delivering performance better than the design goals in terms of reducing the level of interfering SDARS signals in the downstream signal processing paths. Because the existing cryogenic receiver provided a 15 K operating platform, the use of HTS filters was an economical upgrade to the GBT system.

ACKNOWLEDGMENT

The authors would like to thank C. Ansell and D Holdom for their technical support, and S. Ransom of NRAO for the measured pulsar spectrum.

REFERENCES

- [1] NRAO, eNews [Online]. Available: http://www.nrao.edu/news/newsletters/enews/enews_1_7/enews_1_7.shtml
- [2] G. L. Matthaei, L. Young, and E. M. T. Jones, *Microwave Filters Impedance-Matching Networks and Coupling Structure*. Norwood, MA: Artech House, 1980, ch. 12, pp. 725–773.
- [3] G. Zhang, M. J. Lancaster, F. Huang, and N. Roddis, "A superconducting microstrip bandstop filter for an L-band radio telescope receiver," in *Proc. 35th Eur. Microw. Conf.*, Manchester, U.K., 2005, pp. 697–700.
- [4] E. R. Soares, "Design and construction of high performance HTS pseudo-elliptical band-stop filters," in *IEEE MTT-S Int. Dig.*, Jun. 1999, pp. 1555–1558.
- [5] Y. Li, M. J. Lancaster, F. Huang, and N. Roddis, "Superconducting microstrip wide band filter for radio astronomy," in *IEEE MTT-S Int. Dig.*, Jun. 2003, pp. 551–554.
- [6] F. Huang, "Ultra-compact superconducting narrow-band filters using single- and twin-spiral resonators," *IEEE Trans. Microw. Theory Tech.*, vol. 51, no. 2, pp. 487–491, Feb. 2003.
- [7] NRAO, eNews [Online]. Available: <http://www.gb.nrao.edu/electronics/edtn/edtn210.pdf>
- [8] EM User's Manual 9.0 ed. North Syracuse, NY, Sonnet Software Inc., 2004.